

# Evidence for a tumoral immune resistance mechanism based on tryptophan degradation by indoleamine 2,3-dioxygenase

Catherine Uyttenhove<sup>1,3</sup>, Luc Pilotte<sup>1,3</sup>, Ivan Théate<sup>1,2</sup>, Vincent Stroobant<sup>1</sup>, Didier Colau<sup>1</sup>, Nicolas Parmentier<sup>1</sup>, Thierry Boon<sup>1</sup> & Benoît J Van den Eynde<sup>1</sup>

**T lymphocytes undergo proliferation arrest when exposed to tryptophan shortage, which can be provoked by indoleamine 2,3-dioxygenase (IDO), an enzyme that is expressed in placenta and catalyzes tryptophan degradation. Here we show that most human tumors constitutively express IDO. We also observed that expression of IDO by immunogenic mouse tumor cells prevents their rejection by preimmunized mice. This effect is accompanied by a lack of accumulation of specific T cells at the tumor site and can be partly reverted by systemic treatment of mice with an inhibitor of IDO, in the absence of noticeable toxicity. These results suggest that the efficacy of therapeutic vaccination of cancer patients might be improved by concomitant administration of an IDO inhibitor.**

IDO is an enzyme catalyzing the initial and rate-limiting step in the catabolism of tryptophan along the kynurenine pathway<sup>1</sup>. The IDO activity of mouse placenta has an essential role in preventing rejection of allogeneic fetuses<sup>2</sup>. By depleting tryptophan locally, IDO seems to block the proliferation of alloreactive T lymphocytes. T lymphocytes are extremely sensitive to tryptophan shortage, which causes their arrest in the G1 phase of the cell cycle<sup>3</sup>. These observations introduced the concept that IDO expression could suppress immune responses by blocking T-lymphocyte proliferation locally<sup>4–6</sup>. Expression of IDO was also observed in cells exposed to interferon (IFN)- $\gamma$  and in certain types of activated macrophages and dendritic cells, suggesting a role of IDO in the regulation of immune responses<sup>4,7–12</sup>.

Stimulated by these findings, we set out to examine whether IDO is expressed by tumor cells and whether it allows these cells to inhibit T-cell-mediated rejection responses.

## RESULTS

### Constitutive expression of IDO in human tumors

We first observed that many human tumor cell lines express the mRNA of *INDO*, the IDO-encoding gene, constitutively, as detected by real-time RT-PCR (Fig. 1a). To confirm that this constitutive gene expression was associated with the presence of a functionally active protein, we used western blots and enzymatic assays. For western blotting, we used rabbit antibodies raised against a C-terminal peptide of human IDO (Fig. 1b). The purified antibodies stain a band of 40–42 kDa in placenta lysates, consistent with the size of IDO. A band

of the same size was detected in 293 cells after transfection of a human *INDO* cDNA, confirming that it corresponded to IDO. The IDO protein was clearly detected in lysates of a number of tumor cell lines expressing *INDO* mRNA in the absence of IFN- $\gamma$  exposure. The activity of IDO in those tumor lines was confirmed in an enzymatic assay that used high-performance liquid chromatography (HPLC) to measure kynurenine production after incubating the tumor lysates in the presence of tryptophan. All tumor lines that were positive by western blot also contained functionally active IDO (Fig. 1c). The level of IDO activity in the positive lines was in the same range as the placental activity and was much higher in some lines. These results suggest that the IDO activity of some tumor cells is potentially sufficient to mediate substantial effects *in vivo*. We also observed that the *in vitro* growth of some of these tumor lines was improved in the presence of the IDO inhibitor 1-methyl-L-tryptophan (1MT). For instance, the doubling time of melanoma cell line LB1610-MEL was reduced from 135 h to 90 h in the presence of 400  $\mu$ M 1MT.

Because tumor cell lines grown *in vitro* may not represent the exact state of tumor cells *in vivo*, we tested the expression of IDO protein in human tumor samples. We took advantage of the fact that our purified IDO-specific antibodies were able to stain tissue sections. The specificity of the staining was confirmed using 293 cells transfected with *INDO* cDNA (Fig. 2a,b). We tested a large series of human tumors of various origins, most of which contained IDO-positive tumor cells (Table 1). We observed tumor cells expressing IDO in all cases of prostatic, colorectal, pancreatic and cervical carcinomas, as well as in many samples of other tumor types. In all cases, most

<sup>1</sup>Ludwig Institute for Cancer Research and Cellular Genetics Unit, Université de Louvain, B-1200 Brussels, Belgium. <sup>2</sup>Department of Pathology, Université de Louvain, B-1200 Brussels, Belgium. <sup>3</sup>These authors contributed equally to this work. Correspondence should be addressed to B.J.V.d.E. (benoit.vandeneynde@br.u.licr.org).

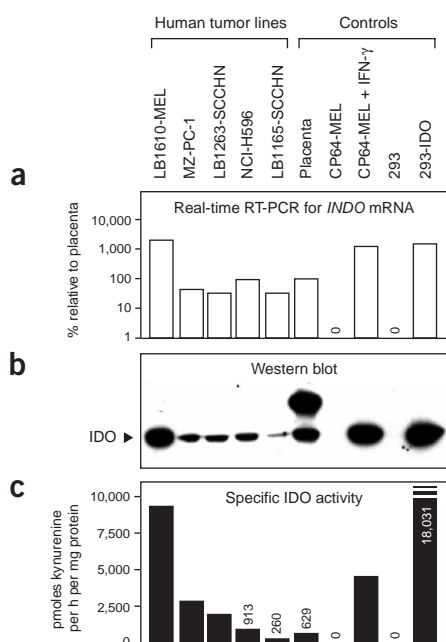


**Figure 1** Constitutive expression and activity of IDO in human cancer cell lines. **(a)** Real-time RT-PCR for *INDO* expression. LB1610-MEL, melanoma line; MZ-PC-1, pancreatic carcinoma; NCI-H596, non-small-cell lung carcinoma; LB1263-SCCHN, laryngeal carcinoma; LB1165-SCCHN, pharyngeal squamous-cell carcinoma. Positive controls were placenta, IDO-transfected 293 cells and IFN- $\gamma$ -treated CP64-MEL melanoma cells. Negative controls were untransfected 293 and untreated CP64-MEL cells. **(b)** Lysates of the same cell lines used in **a** were tested by western blotting using IDO-specific antibodies. The higher molecular weight band of the placenta was also observed when the first antibodies were omitted, and therefore results from a cross-reaction with the secondary antibodies. **(c)** The same lysates as in **b** were tested for IDO activity in an enzymatic assay using HPLC to measure kynurenine production. Data shown is the mean value of three independent assays with similar results.

normal cells of the stroma were negative, suggesting that the IDO expression in the tumor cells did not result from *in vivo* exposure to IFN- $\gamma$ , which would also induce IDO in the stroma. These results indicate that human tumors frequently express IDO *in vivo*. **Figure 2** illustrates the staining of some sections, including a non-small-cell lung carcinoma (**Fig. 2c**), where the staining of tumor cells was abolished by blocking with a synthetic peptide corresponding to the IDO C-terminal sequence, further demonstrating the specificity of the staining. We also show the staining of ovarian, pancreatic and head and neck carcinomas, as well as a lymph node metastasis of a colonic adenocarcinoma (**Fig. 2d–g**). For each sample, we stained an adjacent section with antibodies to cytokeratin-22, confirming the epithelial origin of the tumor cells invading the tissue. Malignancy was determined morphologically by the observation of an infiltrative growth pattern (**Fig. 2c,e,f**), cellular abnormalities (**Fig. 2c,d**), papillary architecture (**Fig. 2d**) and metastasis (**Fig. 2g**). Although in some tumors all cancerous cells were strongly positive for IDO (**Fig. 2d,e**), in others the staining was weaker or more heterogeneous (**Fig. 2c,f,g**). By visual estimation, we grouped the tumors into three categories according to the proportion of tumors cells stained for IDO (**Table 1**). The highest proportions were observed in prostatic, pancreatic and colorectal carcinomas. Besides the tumor cells, we observed the presence of some IDO-positive cells at the periphery of many tumors (**Fig. 2g**). Those cells, which were cytokeratin-22-negative, were usually located within an area enriched in inflammatory cells and might be activated antigen-presenting cells, such as interdigitating dendritic

cells, as suggested by the double staining of some of these cells for IDO and protein S100 (**Fig. 2g**).

### Tumors expressing IDO resist immune rejection

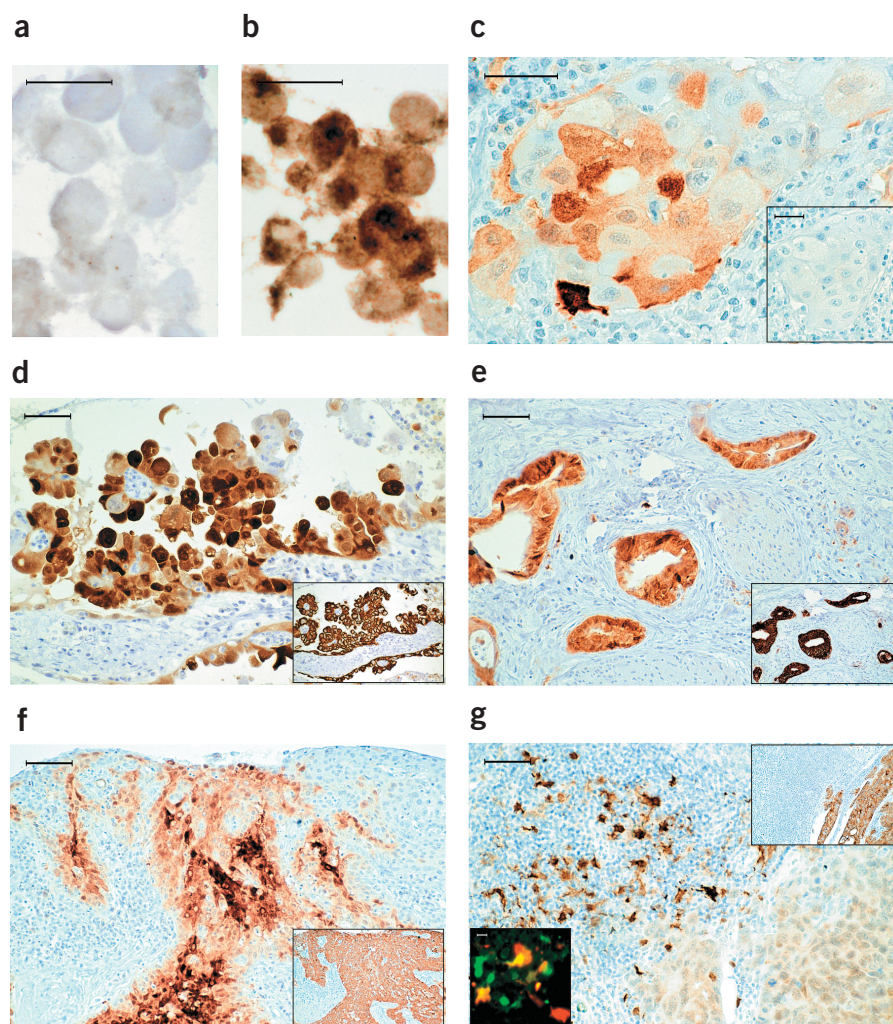
To determine whether constitutive expression of IDO allows tumor cells to avoid immune rejection by T cells, we used the P815 mouse tumor model. P815 tumor cells regularly produce progressive tumors when injected intraperitoneally into naive syngeneic DBA/2 mice, even though they are clearly immunogenic and express several antigens recognized by cytolytic T lymphocytes (CTLs). One of these antigens, P1A, is encoded by the *Trap1a* gene and is the major target of the rejection response in mice immunized against P815 (ref. 13). We previously reported that mice immunized against this antigen reject a challenge of P815 cells injected intraperitoneally<sup>14</sup>. By testing

**Table 1** Expression of IDO in human tumors

Tumor type	IDO-positive tumor samples <sup>a</sup> (no. positive per no. tested)	Proportion of IDO-positive tumor cells <sup>b</sup>		
		>50%	10–50%	<10%
Prostatic carcinomas	11/11	7	3	1
Colorectal carcinomas	10/10	5	3	2
Pancreatic carcinomas	10/10	8	2	0
Cervical carcinomas	10/10	0	4	6
Endometrial carcinomas	5/5	0	3	2
Gastric carcinomas	9/10	4	3	2
Glioblastomas	9/10	6	3	0
Non-small-cell lung carcinomas	9/11	1	1	7
Bladder carcinomas	8/10	3	1	4
Ovarian carcinomas	8/10	0	3	5
Head and neck carcinomas	7/11	0	3	4
Esophageal carcinomas	7/10	1	2	4
Mesotheliomas	6/10	2	1	3
Renal cell carcinomas	5/10	0	1	4
Melanomas	11/25	0	0	11
Breast carcinomas	3/10	2	0	1
Thyroid carcinomas	2/10	0	0	2
Lymphomas	4/18	0	0	4
Small-cell lung carcinomas	2/10	0	0	2
Sarcomas	2/10	0	1	1
Hepatocarcinomas	2/5	0	0	2
Adrenal carcinomas	2/5	1	0	1
Choriocarcinomas	1/5	0	0	1
Cutaneous basocellular carcinomas	1/5	0	0	1
Testicular seminomas	0/10	0	0	0

<sup>a</sup>Expression of IDO protein was detected by immunohistochemistry using purified IDO-specific rabbit antibodies. Specificity of staining was controlled by blocking with a synthetic peptide corresponding to the C terminus of IDO (**Fig. 2**). <sup>b</sup>Number of tumor samples with the indicated proportion of IDO-positive tumor cells is given in each column. The proportion of positive tumor cells was estimated visually.

**Figure 2** Expression of IDO protein in human tumors. (a,b) IDO immunostaining of cultures of untransfected (a) or IDO-transfected (b) 293 cells. (c) Adjacent sections of a non-small-cell lung carcinoma stained in the absence or presence (inset) of IDO-blocking peptide. (d–g) Adjacent sections of an ovarian carcinoma (d), a pancreatic adenocarcinoma (e), a head and neck carcinoma (f) and a lymph node metastasis of colonic adenocarcinoma (g), stained with antibodies to IDO (main panels) or cytokeratin-22 (insets). The smaller inset of g shows double immunofluorescent staining for IDO (red) and protein S100 (green). Scale bar = 100  $\mu$ m (c–g) or 20  $\mu$ m (a–b and g, small inset).



various P815 sublines for expression of *Indo* using real-time RT-PCR, we identified subline P815B, which was completely negative (Table 2), and transfected the P815B cells with an expression plasmid containing the mouse *Indo* cDNA. Transfected cells were cloned by limiting dilution and clones were tested by real-time RT-PCR for expression of *Indo* mRNA. Expression of functional IDO was then confirmed in an enzymatic assay as reported above (Table 2). For the *in vivo* experiments reported below, we selected three clones: clone 6, which expresses very high levels of IDO; clone 7, which has IDO activity similar to that of placenta; and clone 1, which was transfected with a control vector and does not express any IDO.

We then immunized mice against the P1A antigen and injected them 4 weeks later with an intraperitoneal challenge of transfected P815B cells, that either expressed or did not express IDO. As expected, most mice injected with P815B clone 1 completely rejected the tumor challenge. In contrast, the majority of mice injected with IDO-expressing cells developed progressive tumors and died (Fig. 3a). This was true not only for P815B-IDO clone 6, which expressed very high amounts of IDO, but also for clone 7, which expressed a lower level. The three cell lines produced progressive tumors in all naive mice, but the IDO-expressing

tumors grew faster. This is consistent with the notion that in these mice, a primary immune response retards the growth of the P815 tumors but is abolished when the tumors express IDO (Fig. 3b). The progression of IDO-expressing P815 cells in immunized mice and their faster growth in naive mice was not related to a higher intrinsic tumorigenicity, because irradiated naive mice injected with P815B

clone 1 or IDO-transfected clones all developed tumors quickly and with identical kinetics (Fig. 3b). In addition, the *in vitro* growth rate of IDO-positive clone 7 was identical to that of IDO-negative clone 1, and the growth of IDO-positive clone 6 was slower except when an IDO inhibitor was added to the culture medium (Table 2). The three cell lines also expressed identical levels of *Trap1a* mRNA, as measured by RT-PCR (data not shown), and were equally lysed by P1A-specific CTLs (Fig. 3c). Altogether, these results suggested that the progression of the IDO-expressing tumors in the P1A-immunized mice resulted from the ability of those tumors to prevent their rejection by T lymphocytes.

It has been proposed that the resistance of IDO-expressing cells to immune rejection

**Table 2** Expression of IDO in mouse tumor lines used in this study

	Expression of <i>Indo</i> mRNA relative to day 11 placenta (%) <sup>a</sup>	IDO enzymatic activity (pmol kynurenine per h per mg protein) <sup>b</sup>	Doubling time (h) <sup>c</sup>	
			–1MT	+1MT
Placenta day 11	100	284		
Placenta day 18	154	107		
Mastocytoma P815, subline P815B	0	ND	ND	ND
Mastocytoma P815, subline P1HTR	143	ND	ND	ND
Mastocytoma P815, subline P511	35	ND	ND	ND
Transfected P815B cells				
P815B clone 1 (control)	0	0	12.6	12.7
P815B-IDO clone 6	275,887	15,403	18.2	13.0
P815B-IDO clone 7	912	152	12.6	12.9

<sup>a</sup>Expression of mouse *Indo* mRNA was measured by real-time RT-PCR as described in Methods. RNA isolated from total placenta at gestational day 11 was used as a reference. <sup>b</sup>Enzymatic activity was tested on cell lysates as described in Methods. <sup>c</sup>Doubling time was calculated on the basis of twice-weekly cell counts over a 3-week culture period, in the absence or presence of 1MT. <sup>d</sup>ND, not determined.

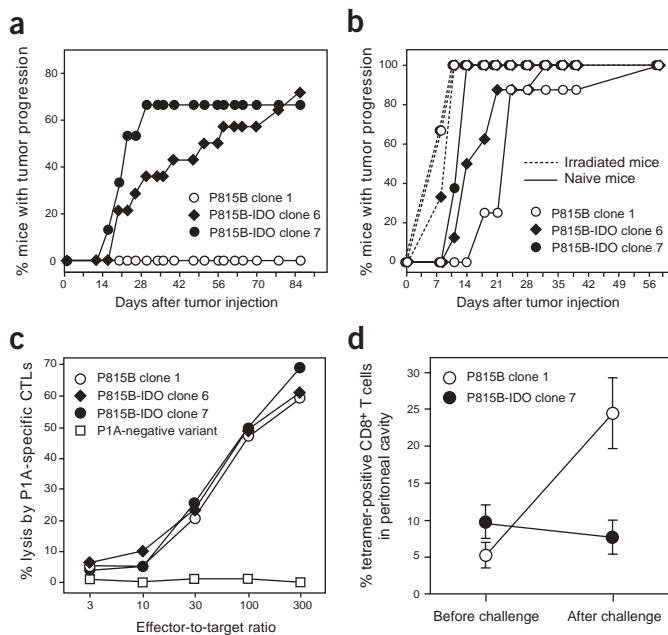


**Figure 3** Immune resistance of IDO-expressing tumors. (a) Immunized mice ( $n = 15$  per group) were challenged by intraperitoneal injection of  $4 \times 10^5$  cells as indicated. One representative experiment out of six is shown. (b) Naive ( $n = 10$  per group) or irradiated mice ( $n = 6$  per group; 650 cGy) were injected as in a. (c) Lysis of IDO-transfected P815B cells by P1A-specific CTLs. P815 variant P1.istA<sup>B</sup>, which has lost gene P1A (ref. 35), was used as a control target. (d) Proportion of P1A-specific T cells in the peritoneal cavities of immunized mice, estimated using H-2L<sup>d</sup>/P1A tetramers 4–7 d before, or 4 d after, intraperitoneal challenge with  $10^6$  cells of P815B clone 1 ( $n = 33$  mice) or P815B-IDO clone 7 ( $n = 31$  mice). Error bars represent s.e.m.  $P = 0.00005$  for clone 1 versus clone 7 after challenge.

results from an arrest of T-cell proliferation caused by local tryptophan depletion<sup>1,3</sup>. We measured the number of P1A-specific CD8<sup>+</sup> T cells present in the peritoneal cavities of immunized mice before and after challenge with P815 tumor cells, using tetramers of H-2L<sup>d</sup> molecules loaded with the P1A antigenic peptide. Immunized mice contained detectable amounts of P1A-specific T cells, in the range of 5–10% of the CD8<sup>+</sup> T cells of the peritoneal cavity. Four days after challenge with P815B clone 1 tumor cells, the proportion of tetramer-positive T cells in the peritoneal cavity had increased by a mean factor of  $6.7 \pm 1.7$ , indicating a strong local accumulation of specific T cells (Fig. 3d). In contrast, after challenge with the IDO-expressing tumor cells of P815B-IDO clone 7, the proportion of P1A-specific T cells in the peritoneal cavity remained the same or decreased (Fig. 3d). Annexin V staining did not reveal significant apoptosis of P1A-specific T cells (data not shown). In blood lymphocytes, the number of P1A-specific T cells was below detectable levels when tested *ex vivo* on fresh cells of mice from all groups. After one week of stimulation *in vitro*, P1A-specific CTL activity was detected in blood lymphocytes and was identical in mice challenged with tumor cells expressing or not expressing IDO (data not shown). These results suggest that IDO-expressing tumors block T-lymphocyte proliferation locally.

#### Pharmacological inhibition of IDO

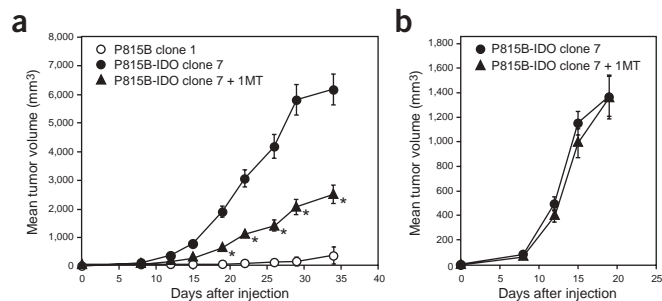
IDO expression is not the only mechanism by which tumors can resist immune rejection<sup>15–17</sup>, but it has the major interest of being amenable to pharmacological intervention. IDO activity can be

inhibited by various tryptophan analogs, including the competitive inhibitor 1MT<sup>18</sup>, which was successfully used *in vivo* to block the immune privilege of placenta<sup>2</sup>.

We therefore tested whether 1MT treatment would prevent the growth of IDO-expressing P815B cells injected into P1A-immunized mice. We used oral administration to reach active levels of 1MT for sustained periods of time. The bioavailability of 1MT delivered by this route was confirmed using HPLC, which measured a mean concentration of 205  $\mu$ M 1MT in the sera of mice receiving 5 mg/ml 1MT in the drinking water, for a mean tryptophan level of 70  $\mu$ M. This serum level of 1MT should be active on mouse IDO, as the inhibition constants of 1MT measured *in vitro* on purified rabbit or human IDO were 7  $\mu$ M and 68  $\mu$ M, respectively<sup>18,19</sup>. We used the same experimental setup as before, except that tumors were injected subcutaneously rather than intraperitoneally to allow monitoring of tumor growth by size measurements. We verified that naive mice injected subcutaneously with  $10^6$  P815B clone 1 cells all developed progressive tumors ( $n = 15$ ; data not shown). As before, P1A-immunized mice completely rejected control P815B clone 1 cells but did not reject IDO-expressing P815B-IDO clone 7 cells (Fig. 4a). However, when mice received 1MT in the drinking water, they rejected IDO-expressing P815B cells more efficiently than untreated mice, as indicated by the significantly slower progression of the tumors (Fig. 4a;  $P \leq 0.00001$ ). Treatment with 1MT did not completely prevent tumor outgrowth, perhaps because of incomplete inhibition of IDO by 1MT or because of variations in 1MT serum levels caused by the irregular drinking that was observed in some mice. Treatment of mice with 1MT was not associated with noticeable toxicity, although mice tended to drink lower amounts of water and were rather dehydrated. To make sure that the reduced tumor progression observed in treated mice was due to the abolition of IDO-mediated immune suppression and not to dehydration or any other effect of 1MT, we repeated the experiment in immune mice that were depleted of T cells before injection of tumor cells and during tumor growth. The progression of IDO-expressing tumor cells was equal in T-cell-depleted mice that were untreated or treated with 1MT (Fig. 4b). This result indicated that the effect of 1MT on tumor progression was not due to dehydration, but rather required T cells and therefore seemed to result from IDO inhibition.

**Figure 4** Reversal of immune resistance by systemic inhibition of IDO.

(a) Mean tumor volumes in immunized mice challenged with subcutaneous injection of  $10^6$  cells of P815B clone 1 ( $n = 15$  mice) or challenged with P815B-IDO clone 7 and treated ( $n = 24$  mice) or not ( $n = 30$  mice) with 1MT in the drinking water. \*,  $P \leq 0.00001$  for treated compared with untreated mice. (b) Mean tumor volumes in immunized mice depleted of T cells by weekly injections of antibodies to CD4 and CD8, starting 2 d before tumor challenge was performed as in a. Mice received either normal drinking water ( $n = 15$  mice) or a solution of 1MT ( $n = 14$  mice). Error bars in a and b represent s.e.m.



## DISCUSSION

IDO is a cytosolic enzyme, so tryptophan degradation by IDO occurs inside the cell<sup>19</sup>. Because tryptophan readily crosses the plasma membrane through specific transporters<sup>20</sup>, a microenvironment depleted of tryptophan is created in the vicinity of IDO-expressing cells, which function as 'tryptophan sinks'<sup>3</sup>. Protein synthesis proceeds despite lowered levels of tryptophan, presumably because the  $K_m$  of tryptophanyl-tRNA synthetase for tryptophan is lower than that of IDO<sup>19,21,22</sup>. This enables most cells to maintain their growth in the presence of IDO. For instance, although tumor cells expressing high levels of IDO have a reduced growth rate *in vitro*, their proliferation is not arrested. T lymphocytes, in contrast, stop proliferating under such conditions because they have a tryptophan-sensitive checkpoint, which blocks their cell cycle in the G1 phase when tryptophan concentration is below 0.5–1  $\mu\text{M}$  (ref. 3).

Recent reports suggest that proliferation arrest caused by tryptophan depletion is not the only mechanism whereby IDO expression may alter T-cell responses. Some tryptophan catabolites induce apoptosis of T cells, primarily of CD4<sup>+</sup> cells<sup>23,24</sup>. In our studies, we saw a lack of accumulation of P1A-specific CD8<sup>+</sup> T cells at the tumor site in the presence of IDO-expressing tumor cells, without signs of T-cell apoptosis. This result favors the model of proliferation arrest of CD8<sup>+</sup> T cells. This was further supported by *in vitro* data showing a reduced proliferation of P1A-specific T cells when stimulated with P815B-IDO clone 7 cells, compared with stimulation with P815B clone 1 cells, again in the absence of apoptosis as measured by staining with annexin V (data not shown).

The molecular definition of human tumor antigens recognized by T cells has allowed the design of cancer immunotherapy protocols, based mainly on vaccination with various antigen formulations<sup>25,26</sup>. Although these clinical trials are still in their early days, some tumor regressions have already been observed<sup>27–31</sup>. However, these tumor responses occur only in a low proportion of patients. There are many potential reasons why tumors are not regressing in the other patients, including the possibility that the vaccine may have been insufficient to induce an immune response in those patients. Tumors might also lose expression of the antigen or develop a variety of immune escape mechanisms<sup>15–17</sup>. The mechanism of tumor resistance described here may be of particular relevance to immunotherapy for at least two reasons. First, it is very frequent: as shown in Table 2, a large majority of human tumors express IDO in a constitutive manner. In addition, because IDO is induced by IFN- $\gamma$ , IDO-negative tumor cells may start expressing IDO when exposed to an inflammatory context such as that resulting from an immune response, so the spectrum of tumors potentially using this resistance mechanism may be even wider. Second, this resistance mechanism can be overcome by systemic inhibition of IDO using tryptophan analogs such as 1MT, which could be administered to cancer patients undergoing immunotherapy. This inhibitor is active on human lymphocytes<sup>3,5</sup>, and we have confirmed that some human antitumor CTL clones proliferate better *in vitro* in the presence of 1MT (data not shown). In addition, 1MT does not inhibit tryptophan dioxygenase, the hepatic enzyme regulating systemic tryptophan levels<sup>32</sup>, which suggests that major side effects might be avoided in humans, at least regarding tryptophan metabolism. However, even though we did not observe serious toxicity in mice treated with 1MT, the safety of such treatment will have to be evaluated carefully in additional preclinical models before it can be included in immunotherapy protocols. The optimal mode of administration also needs to be defined. Our results indicate the

effectiveness of the oral route, which could be improved in humans by using a solid form of 1MT instead of a solution, which is limited in concentration by the poor solubility of 1MT. Alternative IDO inhibitors may be developed in the future and could be more efficient than 1MT, which does not entirely block IDO activity.

## METHODS

**Cell lines.** P815B (gift from P. Chen, Harvard Medical School) is a subline of mastocytoma P815 previously used as a vector-transfected control<sup>33,34</sup>. P815B cells were transfected with expression vector pEF6/V5-His (Invitrogen) containing the mouse *Indo* open reading frame, and selected with 5  $\mu\text{g}/\text{ml}$  Blasticidin (Invitrogen) and 200  $\mu\text{M}$  1MT (Sigma-Aldrich). Control cells were transfected with plasmid pEF6/V5-His-LacZ. Cell lines P1.HTR, P511, P1.istA<sup>-</sup>B<sup>-</sup> and L1210.P1A.B7-1 were previously described<sup>14,35,36</sup>. Human 293-EBNA cells (Invitrogen) transfected with expression vector pEF6/V5-His containing the human *INDO* open reading frame were similarly selected. An IDO-positive clone was selected and used in all experiments. The human *INDO* open reading frame was amplified from placenta RNA by RT-PCR using sense primer 5'-GAGGAGCAGACTCAAGAATG-3' and antisense primer 5'-GCATACAGATGTCTCTGCTATG-3'. The mouse *Indo* open reading frame was amplified from placenta RNA using sense primer 5'-GCCAAGTGGGGGTCAGTGGAGTAGACA-3' and antisense primer 5'-GCCCTGATAGAAGTGGAGCTTGCTACTACTA-3'.

**Mice.** DBA/2 mice (14–21 weeks old) were raised in specific pathogen-free conditions, immunized by injecting 10<sup>6</sup> live L1210.P1A.B7-1 cells into the peritoneal cavity<sup>14</sup> once (Fig. 3) or twice (Fig. 4), and challenged 4 weeks later. Mice were given 1MT (Sigma-Aldrich) in the drinking water (5 mg/ml, pH 9.9), of which they drank an average of 3.5 ml/d. Over the whole series of experiments, 2 of 877 untreated mice and 8 of 186 mice given 1MT died without apparent tumors. The eight mice in the latter group apparently died from dehydration resulting from lower fluid intake. For depletion of T cells, mice were injected intraperitoneally with 1 mg each of monoclonal antibodies to CD4 (GK1.5) and CD8 (53-6.72) every week. The efficacy of CD4 and CD8 depletion was verified by staining peripheral blood leukocytes of similarly injected control mice. All mouse experiments were approved by the ethical committee of the Faculty of Medicine, Université de Louvain.

**Lysis assay.** Chromium release assay was done in 4 h as described<sup>35</sup>, using CTLs derived from splenocytes of immunized mice restimulated 1 week *in vitro* with irradiated L1210.P1A.B7-1 cells. A 50-fold excess of unlabeled P1.istA<sup>-</sup>B<sup>-</sup> cells was added to all targets as competitor cells.

**Tetramer staining and fluorescence-activated cell sorting analysis.** H-2L<sup>d</sup>/P1A tetramers were produced as previously described<sup>37</sup>. Peritoneal cells were stained for 15 min at room temperature in PBS buffer containing 1% BSA, 0.1  $\mu\text{M}$  phycoerythrin-labeled H-2L<sup>d</sup>/P1A tetramer and FITC-conjugated antibody to Fc- $\gamma$  receptor III. Peridinin chlorophyll protein-conjugated antibody to CD8 and FITC-conjugated antibodies to CD4, CD11b and CD19 (all from BD PharMingen) were added for an additional incubation of 15 min. Cells were analyzed on a FACScan flow cytometer (BD Biosciences). The CD8-positive and FITC-negative cells were gated.

**Real-time RT-PCR analysis of mRNA expression.** We obtained cDNA as described<sup>38</sup> and amplified it on an ABI PRISM 7700 (PE Applied Biosystems) using the qPCR Core Kit (Eurogentec). For human *INDO*, we used sense primer 5'-GGTCATGGAGATGTCCGTAA-3', antisense primer 5'-ACCAATAGAGAGACCAGGAAGAA-3' and probe FAM-5'-CTGTTCTTACTGCCAAGTCTCCAAGAACTG-3'-TAMRA. For mouse *Indo*, we used sense primer 5'-GTACATCACCATGGCGTATG-3', antisense primer 5'-CGAGGAAGAAGCCCTTGTC-3' and probe FAM-5'-CTGCCCCGCAATATTGCTGTTCCCTAC-3'-TAMRA. For references, we quantified human or mouse  $\beta$ -actin. Cycling conditions were 50 °C for 5 s and 95 °C for 10 min, followed by 45 cycles of 95 °C for 15 s and 60 °C for 1 min.

**Antibodies and western blotting.** We raised a rabbit antiserum against human IDO peptides KTVRSTTEKSLKEG (C-terminal position 389–403)

and QPKENKTSKEDPSKLE (361–375) coupled to keyhole limpet hemocyanin (Eurogentec). The antiserum was purified by affinity chromatography using the C-terminal IDO peptide. Western blotting was done with 15 µg of total protein, estimated using a BCA assay (Pierce). The samples were boiled in SDS with 2% dithiothreitol (20 mM), separated on NuPAGE 10% gels (Invitrogen) and transferred onto a Hybond-C extra membrane (Amersham). The membranes were probed overnight with IDO-specific antibodies, then for 1 h with horseradish peroxidase-linked antibody to rabbit Ig (BD Transduction Laboratories) and revealed by chemiluminescence (SuperSignal, Pierce).

**Enzymatic assay for IDO activity.** We modified a protocol<sup>19</sup> by lowering tryptophan concentration to 80 µM and measuring kynurenine by HPLC on a reverse-phase C18 column.

**Immunohistochemistry.** Samples of neoplastic lesions were selected from archival material, fixed in 10% formalin or Bouin fixative and embedded in paraffin. Sections (5 µm) were deparaffined in xylene, rehydrated and cooked in a double boiler in 0.01 M citrate (pH 5.8) and 0.05% Triton X-100 for 75 min. Endogenous peroxidase was blocked with 0.3% H<sub>2</sub>O<sub>2</sub> for 30 min and nonspecific staining was prevented by preincubation in 10% goat serum for 30 min. Sections were incubated overnight at 4 °C with either purified IDO-specific antibodies (1:300 dilution) or mouse antibodies to human cytokeratin-22 (1:400; Biomedica) and stained using the Envision System (Dako) with diaminobenzidine (Sigma-Aldrich). We also grew 293 cells on culture slides, fixed them in 10% formalin and cooked and stained as above. Peptide blocking was done by adding 1 mg/ml of peptide to the antibodies 30 min before staining. Double staining for IDO and protein S100 was done overnight at 4 °C with a mixture of IDO antibodies (1:70) and mouse antibodies to protein S100 (1:30; NeoMarkers) after blocking endogenous biotin. The sections were then treated with biotin-conjugated antibody to rabbit IgG (1:200; Chemicon), amplified with biotinylated tyramine and incubated with Texas red-streptavidin (1:50; Zymed Laboratories) and FITC-conjugated goat antibody to mouse Ig (Dako).

**Statistics.** We used the two-tailed Student *t*-test for statistical analyses.

#### ACKNOWLEDGMENTS

We thank J. Bilsborough, S. Buonocore, F. Brasseur, P. Camby, D. Donckers, C. Jacques, B. Lethé, F. Piette and G. Warnier for help at various steps of the work; S. Depelchin for editorial assistance; and P. Coulie and P. van der Bruggen for critical reading of the manuscript. This work was supported in part by a grant from FB Assurances and VIVA (Belgium), and by grants QLG1-CT-1999-00622, QLK2-CT-1999-00556 and QLK2-CT-1999-00318 from the Fifth Framework programme of the European Community.

#### COMPETING INTERESTS STATEMENT

The authors declare that they have no competing financial interests.

Received 15 July; accepted 28 August 2003

Published online at <http://www.nature.com/naturemedicine/>

- Mellor, A.L. & Munn, D.H. Tryptophan catabolism and T-cell tolerance: immunosuppression by starvation? *Immunol. Today* **20**, 469–473 (1999).
- Munn, D.H. *et al.* Prevention of allogeneic fetal rejection by tryptophan catabolism. *Science* **281**, 1191–1193 (1998).
- Munn, D.H. *et al.* Inhibition of T cell proliferation by macrophage tryptophan catabolism. *J. Exp. Med.* **189**, 1363–1372 (1999).
- Hwu, P. *et al.* Indoleamine 2,3-dioxygenase production by human dendritic cells results in the inhibition of T cell proliferation. *J. Immunol.* **164**, 3596–3599 (2000).
- Kudo, Y., Boyd, C.A., Sargent, I.L. & Redman, C.W. Tryptophan degradation by human placental indoleamine 2,3-dioxygenase regulates lymphocyte proliferation. *J. Physiol.* **535**, 207–215 (2001).
- Fruento, G., Rotondo, R., Tonetti, M. & Ferrara, G.B. T cell proliferation is blocked by indoleamine 2,3-dioxygenase. *Transplant. Proc.* **33**, 428–430 (2001).
- Fallarino, F. *et al.* Functional expression of indoleamine 2,3-dioxygenase by murine CD8 $\alpha^+$  dendritic cells. *Int. Immunol.* **14**, 65–68 (2002).
- Takikawa, O., Kuroiwa, T., Yamazaki, F. & Kido, R. Mechanism of interferon-gamma action. Characterization of indoleamine 2,3-dioxygenase in cultured human cells induced by interferon-gamma and evaluation of the enzyme-mediated tryptophan degradation in its anticellular activity. *J. Biol. Chem.* **263**, 2041–2046 (1988).
- Habara-Ohkubo, A., Takikawa, O. & Yoshida, R. Cloning and expression of a cDNA encoding mouse indoleamine 2,3-dioxygenase. *Gene* **105**, 221–227 (1991).
- Munn, D.H. *et al.* Potential regulatory function of human dendritic cells expressing indoleamine 2,3-dioxygenase. *Science* **297**, 1867–1870 (2002).
- Friberg, M. *et al.* Indoleamine 2,3-dioxygenase contributes to tumor cell evasion of T cell-mediated rejection. *Int. J. Cancer* **101**, 151–155 (2002).
- Grohmann, U. *et al.* CTLA-4-Ig regulates tryptophan catabolism *in vivo*. *Nature Immunol.* **3**, 1097–1101 (2002).
- Van den Eynde, B., Lethé, B., Van Pel, A., De Plaen, E. & Boon, T. The gene coding for a major tumor rejection antigen of tumor P815 is identical to the normal gene of syngeneic DBA/2 mice. *J. Exp. Med.* **173**, 1373–1384 (1991).
- Brändle, D. *et al.* The shared tumor-specific antigen encoded by mouse gene *P1A* is a target not only for cytolytic T lymphocytes but also for tumor rejection. *Eur. J. Immunol.* **28**, 4010–4019 (1998).
- Medema, J.P. *et al.* Blockade of the granzyme B/perforin pathway through over-expression of the serine protease inhibitor PI-9/SPI-6 constitutes a mechanism for immune escape by tumors. *Proc. Natl. Acad. Sci. USA* **98**, 11515–11520 (2001).
- Pawelec, G. *et al.* Escape mechanisms in tumor immunity: a year 2000 update. *Crit. Rev. Oncog.* **11**, 97–133 (2000).
- Marincola, F., Jaffee, E.M., Hicklin, D.J. & Ferrone, S. Escape of human solid tumors from T-cell recognition: molecular mechanisms and functional significance. *Adv. Immunol.* **74**, 181–273 (2000).
- Cady, S.G. & Sono, M. 1-Methyl-DL-tryptophan,  $\beta$ -(3-benzofuranyl)-DL-alanine (the oxygen analog of tryptophan), and  $\beta$ -13-benzo(b)thienyl-DL-alanine (the sulfur analog of tryptophan) are competitive inhibitors for indoleamine 2,3-dioxygenase. *Arch. Biochem. Biophys.* **291**, 326–333 (1991).
- Kudo, Y. & Boyd, C.A. Human placental indoleamine 2,3-dioxygenase: cellular localization and characterization of an enzyme preventing fetal rejection. *Biochim. Biophys. Acta* **1500**, 119–124 (2000).
- Kudo, Y. & Boyd, C.A. Characterisation of L-tryptophan transporters in human placenta: a comparison of brush border and basal membrane vesicles. *J. Physiol.* **531**, 405–416 (2001).
- Prætorius-Ibba, M. *et al.* Ancient adaptation of the active site of tryptophanyl-tRNA synthetase for tryptophan binding. *Biochemistry* **39**, 13136–13143 (2000).
- Jorgensen, R., Sogaard, T.M.M., Rossing, A.B., Martensen, P.M. & Justesen, J. Identification and characterization of human mitochondrial tryptophanyl-tRNA synthetase. *J. Biol. Chem.* **275**, 16820–16826 (2000).
- Terness, P. *et al.* Inhibition of allogeneic T cell proliferation by indoleamine 2,3-dioxygenase-expressing dendritic cells: mediation of suppression by tryptophan metabolites. *J. Exp. Med.* **196**, 447–457 (2002).
- Fallarino, F. *et al.* T cell apoptosis by tryptophan catabolism. *Cell Death Differ.* **9**, 1069–1077 (2002).
- Van den Eynde, B. & van der Bruggen, P. T cell-defined tumor antigens. *Curr. Opin. Immunol.* **9**, 684–693 (1997).
- Boon, T. & Van den Eynde, B. Tumor immunology—editorial overview. *Curr. Opin. Immunol.* **15**, 129–130 (2003).
- Nestle, F.O. *et al.* Vaccination of melanoma patients with peptide- or tumor lysate-pulsed dendritic cells. *Nat. Med.* **4**, 328–332 (1998).
- Rosenberg, S.A. *et al.* Immunologic and therapeutic evaluation of a synthetic peptide vaccine for the treatment of patients with metastatic melanoma. *Nat. Med.* **4**, 321–327 (1998).
- Marchand, M. *et al.* Tumor regressions observed in patients with metastatic melanoma treated with an antigenic peptide encoded by gene *MAGE-3* and presented by HLA-A1. *Int. J. Cancer* **80**, 219–230 (1999).
- Thurner, B. *et al.* Vaccination with MAGE-3A1 peptide-pulsed mature, monocyte-derived dendritic cells expands specific cytotoxic T cells and induces regression of some metastases in advanced stage IV melanoma. *J. Exp. Med.* **190**, 1669–1678 (1999).
- Jäger, E. *et al.* Induction of primary NY-ESO-1 immunity: CD8 $^+$  T lymphocyte and antibody responses in peptide-vaccinated patients with NY-ESO-1 $^+$  cancers. *Proc. Natl. Acad. Sci. USA* **97**, 12198–12203 (2000).
- Suzuki, S. *et al.* Expression of indoleamine 2,3-dioxygenase and tryptophan 2,3-dioxygenase in early concepti. *Biochem. J.* **355**, 425–429 (2001).
- Uno, T., Chen, P.W., Murray, T.G., Podack, E.R. & Ksander, B.R. Gene transfer of the CD80 costimulatory molecule into ocular melanoma cells using a novel episomal vector. *Invest. Ophthalmol. Vis. Sci.* **38**, 2531–2539 (1997).
- Wenkel, H., Chen, P.W., Ksander, B.R. & Streilein, J.W. Immune privilege is extended, then withdrawn, from allogeneic tumor cell grafts placed in the sub-retinal space. *Invest. Ophthalmol. Vis. Sci.* **40**, 3202–3208 (1999).
- Lethé, B., Van den Eynde, B., Van Pel, A., Corradin, G. & Boon, T. Mouse tumor rejection antigens P815A and P815B: two epitopes carried by a single peptide. *Eur. J. Immunol.* **22**, 2283–2288 (1992).
- Van Pel, A., De Plaen, E. & Boon, T. Selection of a highly transfectable variant from mouse mastocytoma P815. *Som. Cell Genet.* **11**, 467–475 (1985).
- Bilsborough, J. *et al.* TNF-mediated toxicity after massive induction of specific CD8 $^+$  T cells following immunization of mice with a tumor-specific peptide. *J. Immunol.* **169**, 3053–3060 (2002).
- Van den Eynde, B. *et al.* A new family of genes coding for an antigen recognized by autologous cytolytic T lymphocytes on a human melanoma. *J. Exp. Med.* **182**, 689–698 (1995).

